

Metallomics

rsc.li/metallomics



ISSN 1756-591X



ROYAL SOCIETY
OF CHEMISTRY

PAPER

Milena B. P. Soares *et al.*

Platinum(II)–chloroquine complexes are antimalarial agents against blood and liver stages by impairing mitochondrial function

Indexed in
Medline!



Cite this: *Metallomics*, 2017, 9, 1548

Platinum(II)–chloroquine complexes are antimalarial agents against blood and liver stages by impairing mitochondrial function†

Tais S. Macedo,^{‡a} Wilmer Villarreal,^{§b} Camila C. Couto,^a Diogo R. M. Moreira,^{ib a} Maribel Navarro,^c Marta Machado,^d Miguel Prudêncio,^d Alzir A. Batista^b and Milena B. P. Soares^{ib *ae}

Chloroquine is an antimalarial agent with strong activity against the blood stage of *Plasmodium* infection, but with low activity against the parasite's liver stage. In addition, the resistance to chloroquine limits its clinical use. The discovery of new molecules possessing multistage activity and overcoming drug resistance is needed. One possible strategy to achieve this lies in combining antimalarial quinolones with the pharmacological effects of transition metals. We investigated the antimalarial activity of four platinum(II) complexes composed of chloroquine and phosphine ligands, denoted as WV-90, WV-92, WV-93 and WV-94. In comparison with chloroquine, the complexes were less potent against the chloroquine-sensitive 3D7 strain but they were as active as chloroquine in inhibiting the chloroquine-resistant W2 strain of *P. falciparum*. Regarding selectivity, the complexes WV-90 and WV-93 displayed higher indexes. Unlike chloroquine, the complexes act as irreversible parasitocidal agents against trophozoites and the WV-93 complex displayed activity against the hepatic stage of *P. berghei*. The *in vivo* suppression activity against *P. berghei* in the Peters 4 day test displayed by the complexes was similar to that of chloroquine. However, the efficacy in an established *P. berghei* infection in the Thompson test was superior for the WV-93 complex compared to chloroquine. The complexes' antimalarial mechanism of action is initiated by inhibiting the hemozoin formation. While chloroquine efficiently inhibits hemozoin, parasites treated with the platinum complexes display residual hemozoin crystals. This is explained since the interaction of the platinum complexes with ferriprotoporphyrin is weaker than that of chloroquine. However, the complexes caused a loss of mitochondrial integrity and subsequent reduction in mitochondrial activity, and their effects on mitochondria were more pronounced than those in the chloroquine-treated parasites. The dual effect of the platinum complexes may explain their activity against the hemozoin-lacking parasites (hepatic stage), where chloroquine has no activity. Our findings indicate that the platinum(II)–chloroquine complexes are multifunctional antimalarial compounds and reinforce the importance of metal complexes in antimalarial drug discovery.

Received 4th July 2017,
Accepted 19th September 2017

DOI: 10.1039/c7mt00196g

rsc.li/metallomics

^a FIOCRUZ, Instituto Gonçalo Moniz, CEP 40296-710, Salvador, BA, Brazil.

E-mail: milena@bahia.fiocruz.br; Fax: +55 71-31762292

^b UFSCAR, Departamento de Química, 13565-905, São Carlos, SP, Brazil

^c UFJF, ICE, Departamento de Química, 36036-900, Juiz de Fora, MG, Brazil

^d Instituto de Medicina Molecular, Faculdade de Medicina, Universidade de Lisboa, 1649-028 Lisboa, Portugal

^e Centro de Biotecnologia e Terapia Celular, Hospital São Rafael, 41253-190, Salvador, BA, Brazil

† Electronic supplementary information (ESI) available: Compound stability, activity of metallic precursors, hemolysis assay and transmission electron micrographs described are available. See DOI: 10.1039/c7mt00196g

‡ Tais S. Macedo and Wilmer Villarreal share first authorship.

1. Introduction

Malaria is a widespread infectious disease caused by five different human *Plasmodium* species, which mostly affect the Sub-Saharan Africa, Southeast Asia and Latin America populations.¹ The employment of insecticide-treated bed nets in epidemic areas,^{2,3} along with rapid diagnosis⁴ and implementation of artemisinin-based combination therapies,^{5,6} has substantially decreased the spread of the disease in the last three decades. However, reports of decreasing parasite sensitivity to artemisinin-based therapies, mainly in Southeast Asia,⁷ indicate the urgent requirement for the development of novel antimalarial drugs.

Two well-established antimalarial therapeutic targets are the hemoglobin-derived iron ferriprotoporphyrin IX (heme)^{8–10} and

the mitochondrial electron transport chain.¹¹ Crystallization of heme into the insoluble pigment hemozoin takes place in the digestive vacuole of trophozoites.⁹ Chloroquine and other 4-aminoquinolines, such as mefloquine and amodiaquine, achieve antiparasitic activity by impairing hemozoin biosynthesis. An important advantage of this target is its absence in humans. Given the fact that hemozoin formation is restricted to the blood stage of infection, antimalarial drug discovery based on hemozoin inhibitors results in compounds with a limited spectrum of action.¹⁰

The mitochondrial electron transport chain of *Plasmodium* sp. is its only pathway to regenerate ubiquinone (coenzyme Q10), making this pathway crucial for parasite survival¹¹ not only in the blood but also in the liver and sexual parasite stages.¹² The electron transport chain is mainly composed of cytochrome *bc1* complex III and dihydroorotate dehydrogenase. The naphthoquinone atovaquone, an approved antimalarial drug, acts by blocking the *bc1* complex of the mitochondrial electron transport chain of *Plasmodium* sp.^{13,14}

In recent years, the discovery of novel antimalarial agents with multistage activity has been possible, in part, by approaching these two therapeutic targets.¹⁵ Quinolones and quinones are often employed within drug design, providing successful antimalarial drug candidates with multi-stage activities.¹⁶ The design of aminoquinoline derivatives, including chloroquine, has demonstrated the possibility of modifying the structure of this class of compounds towards improving their spectrum of action.^{17–20} We recently showed that organoruthenium complexes containing chloroquine in their composition presented *in vitro* and *in vivo* antimalarial activity. These organoruthenium complexes affected trophozoites by inhibiting hemozoin formation and producing reactive oxygen species (ROS) but, unlike chloroquine, they exhibited fast parasitocidal activity against blood stages and reduced viability of gametocytes.²¹ To advance the knowledge of antiparasitic metal complexes, we now examined in great detail a class of recently discovered platinum(II) complexes containing chloroquine and phosphine ligands in their composition.

2. Materials and methods

2.1 Drugs and dilutions

Platinum(II)–chloroquine complexes (WV-90, WV-92, WV-93, WV-94) and the respective complexes lacking chloroquine (WV-48, WV-31, WV-51, WV-50) were prepared as previously described.²² Chloroquine, mefloquine and artesunate were supplied by FarManguinhos (Rio de Janeiro, Brazil). Primaquine was purchased from Sigma-Aldrich (St. Louis, MO). All the drugs were dissolved in DMSO (PanReac, Barcelona, Spain) prior to use, and then diluted in culture medium. The final concentration of DMSO was less than 0.5% in all the *in vitro* experiments.

2.2 Drug stability

The stability of the platinum complexes in solution was monitored using the ³¹P{¹H} technique, where a solution of the platinum(II)–chloroquine complexes in a mixture DMSO:Trizma 60:40 was

analyzed on a 9.4 T Bruker Advance III NMR spectrometer at 0, 24, 48, 72 and 216 h.

2.3 Animals

Male Swiss Webster mice (4–6 weeks) were housed at Instituto Gonçalo Moniz (Fiocruz, Bahia, Brazil), maintained in sterilized cages under a controlled environment, receiving a rodent balanced diet and water *ad libitum*. All the experiments were carried out in accordance with the recommendations of Ethical Issues Guidelines and were approved by the local Animal Ethics Committee (protocol number 02/2016).

2.4 Cell culture

CQ-sensitive 3D7 and CQ-resistant W2 strains of *P. falciparum* were cultivated in human O⁺ erythrocytes (donated by HEMOBA, Salvador, Brazil) at 5% hematocrit with daily maintenance in Roswell Park Memorial Institute medium (RPMI-1640, Sigma-Aldrich) supplemented with 10% (v/v) heat-inactivated human plasma (donated by HEMOBA, Salvador, Brazil), 25 mM 4-(2-hydroxyethyl)-1-piperazineethanesulfonic acid (HEPES, Chem-Cruz, Dallas, TX), 300 μM hypoxanthine (MP Biomedicals, Santa Ana, CA), 11 mM glucose (Sigma-Aldrich) and 20 μg mL⁻¹ of gentamicin (Life, Carlsbad, CA). Five days prior to use, *P. falciparum* was cultivated without hypoxanthine and synchronized to rings by 5% D-sorbitol (USB, Santa Clara, CA). The NK65 strain of *P. berghei* was routinely maintained in Swiss mice prior to use in the experiments. The transgenic *P. berghei* expressing green fluorescent protein (GFP) and firefly luciferase (Luc), (*PbGFP-Luccon*, parasite line 676m1cl1) were freshly obtained through the disruption of salivary glands of infected female *Anopheles stephensi* mosquitoes. Human hepatoma cell line Huh-7 was cultured in RPMI-1640 medium supplemented with 10% (v/v) fetal bovine serum, 1% (v/v) nonessential amino acids, 1% (v/v) penicillin/streptomycin, 1% (v/v) glutamine, and 10 mM HEPES. J774 macrophages were cultured in Dulbecco's modified Eagle's medium (DMEM) (Sigma-Aldrich) supplemented with 10% (v/v) heat-inactivated fetal bovine serum (FBS, Gibco, Gaithersburg, MD) and 50 μg mL⁻¹ of gentamicin (Life). Hepatocellular carcinoma cells (HepG2) were cultivated in RPMI-1640 supplemented with 10% (v/v) heat-inactivated FBS and 50 μg mL⁻¹ of gentamicin (Life).

2.5 Cell toxicity

In 96-well plates, the HepG2 or J774 cells were seeded (1.0 × 10⁴ per well) in 100 μL of RPMI and DMEM, respectively. Drugs were added 24 h later in a volume of 100 μL suspended in the medium and the plates were incubated for 72 h at 37 °C and 5% CO₂. Drugs were tested in eight concentrations (150–0.78 μM), each one in triplicate. Gentian violet (Synth, Diadema, Sao Paulo, Brazil) was used as a positive control, while the untreated cells were employed as negative controls. Then, 20 μL of AlamarBlue (Life) was added and the plates were incubated for 4–6 h. Colorimetric readings were performed at 570 and 600 nm using a SpectraMAX 190 instrument (Molecular Devices, Sunnyvale, CA). The mean CC₅₀ values were calculated using data from three independent experiments.

2.6 Hemolysis assay

Fresh uninfected human O⁺ erythrocytes were washed three times with sterile phosphate-buffered saline (PBS), adjusted for 1% hematocrit and 100 μ L was dispensed in a 96-well round bottom plate. Then, 100 μ L of drugs previously in DMSO and suspended in PBS were dispensed in the respective wells. Each drug was tested in seven concentrations (100–1.5 μ M), assayed in triplicate. The untreated cells received 100 μ L of PBS containing 0.5% (v/v) DMSO (negative control), while positive controls received saponin (Sigma-Aldrich) at 1% v/v. The plates were incubated for 1 h at 37 °C under 5% CO₂. The plates were centrifuged at 1500 rpm for 10 min and 100 μ L of the supernatant were transferred to another plate, in which absorbance at 540 nm was measured using a SpectraMax 190 instrument. The percentage of hemolysis was calculated in comparison with positive and negative controls, and plotted against drug concentration generated using GraphPad Prism 5.01. Two independent experiments were performed.

2.7 Cytostatic activity for *P. falciparum* blood stage

One hundred μ L of rings at 1% parasitemia and 2.5% hematocrit in RPMI were dispensed in a 96-well round bottom plate. Then, 100 μ L of drugs (4.0–0.003 μ M) previously suspended in RPMI was dispensed in the respective wells. Each drug was tested in triplicate, in seven different concentrations. The untreated parasite samples received 100 μ L of medium containing 0.5% DMSO. Chloroquine was used as a positive control. The plates were incubated for 24 h at 37 °C under 3% O₂, 5% CO₂ and 91% N₂ atmosphere. Then, 25 μ L of tritiated hypoxanthine (0.5 μ Ci per well, PerkinElmer, Shelton, CT) in RPMI was added to each well and incubated for 24 h. The plates were frozen at –20 °C and subsequently thawed and the contents transferred to UniFilter-96 GF/B PEI coated plates (PerkinElmer) using a cell harvester. After drying, 50 μ L of scintillation cocktail (MaxiLight, Hidex, Turku, Finland) was added in each well and sealed and the plate was read in a liquid scintillation microplate counter (Chameleon, Turku, Finland). The % of inhibition was determined in comparison with untreated cells and the inhibitory concentration for 50% (IC₅₀) values were determined by using non-linear regression with the Logistic equation available in OriginPro 8.5. Three independent experiments were performed.

2.8 Cytotoxic activity for *P. falciparum* blood stage

One hundred μ L of trophozoites of W2 strain at 2% parasitemia and 3.0% hematocrit in RPMI were dispensed in a 96-well round bottom plate. Then, 100 μ L of drugs (10–0.07 μ M) previously suspended in RPMI was added to the respective wells. Each drug was tested in seven concentrations, each one in triplicate. The untreated parasites received 100 μ L of medium containing 0.5% (v/v) DMSO, and artesunate was used as a positive control. The plates were incubated for 18 h at 37 °C under 3% O₂, 5% CO₂ and 91% N₂ atmosphere. The plate was centrifuged three times with 200 μ L of drug-free medium at 1500 rpm for 5 min, then 200 μ L of medium containing tritiated hypoxanthine was added and the plate was incubated for 48 h.

The plates were frozen at –20 °C and thawed and transferred to UniFilter-96 GF/B PEI coated plates (PerkinElmer) using a cell harvester. After drying, 50 μ L of scintillation cocktail was added to each well, and sealed and the plate was read using a liquid scintillation microplate counter. The IC₅₀ values were determined employing non-linear regression with the Logistic equation available in the OriginPro 8.5 software. Minimal parasitocidal concentration (MPC) was determined as the concentration that reduces parasite growth by 99 \pm 1.0%. Three independent experiments were performed.

2.9 Effects on *P. falciparum* cell cycle

A volume of 100 μ L of rings of *P. falciparum* 3D7 strain at 2% parasitemia and 2.5% hematocrit in RPMI was dispensed per well in 96-well round bottom plates. Then, 100 μ L of drugs previously suspended in RPMI was added to the respective wells. Each drug concentration was tested in triplicate. Untreated parasites received 100 μ L of medium containing 0.5% (v/v) DMSO. The plates were incubated for 48 h at 37 °C under 3% O₂, 5% CO₂, 91% N₂ atmosphere followed by centrifugation three times with 200 μ L of drug-free medium at 1500 rpm for 5 min. A volume of 200 μ L of medium containing drugs was added and the plates were incubated for an additional 48 h. Thin blood smears were then prepared, fixed and stained with quick panoptic stain (Laborclin, Pinhais, Brazil). The slides were observed in an optical microscope (CX41, Olympus, St. Louis, MO). The numbers of rings, trophozoites and schizonts were counted in at least 1500 cells per slide ($n = 4$) and plotted against drug concentration generated using GraphPad Prism 5.01. Two independent experiments were performed.

2.10 Interaction with ferriprotoporphyrin²³

A stock solution of 3.5 mg of hemin (Sigma-Aldrich) in 10 mL DMSO was prepared. The solutions of Fe^{III}PPIX (40% v/v DMSO pH 7.5) were prepared daily by mixing 140 μ L stock solution with 3.68 mL DMSO, 1 mL 0.2 M trizma buffer (pH 7.5) and 5 mL doubly distilled deionized water. Aliquots of 5 μ L of platinum-chloroquine solution (at 0.5 mM) were added to a quartz cell containing 2 mL of Fe^{III}PPIX solution (40% v/v DMSO pH 7.5). The absorbance was recorded at 402 nm using a Hewlett Packard spectrophotometer, diode array model 8452. The reference cell containing 2 mL of 40% v/v DMSO solution, and 0.02 M trizma pH 7.5 containing platinum(II) chloroquine solutions was also titrated in order to subtract the absorbance of the drug. The binding affinities were obtained using the equation $A = (A_0 + A_\infty K[C]) / (1 + K[C])$ for a 1:1 complexation model using nonlinear least squares fitting where A_0 is the absorbance of hemin before the addition of complex or free chloroquine, A_∞ is the absorbance for the drug-hemin adduct at saturation, A is the absorbance at each point of the titration, and K is the conditional association constant. Three independent experiments were performed.

2.11 Inhibition of β -hematin formation by infrared spectroscopy⁸

The transformation of hemin into β -hematin in acidic acetate solutions was studied by the reaction of 12 mg hemin

(Sigma-Aldrich) in 3 mL of 0.1 N NaOH, 0.3 mL of 0.1 M HCl and 1.7 mL of 10 M acetate buffer (pH 5), incubated at 60 °C during all the experiments. In a control test, after 0, 30, 60 and 120 min, 1 mL of solution was collected, cooled on ice for 10 min and then filtered over cellulose acetate (0.22 µm). The solids were washed with water, and dried in silica gel and P₂O₅ for 48 h. Infrared spectra were obtained from the discs of the solids in KBr pellets. The effect of the compounds was studied by adding 3 equivalents (mol mol⁻¹) of compounds before the acidification stage, and the reaction was terminated after 120 min. Chloroquine and Primaquine were used as positive and negative controls, respectively. Three independent experiments were performed.

2.12 Inhibition of β-hematin formation by UV-vis spectroscopy²⁴

A solution of hemin chloride (50 µL, 4 mM) dissolved in DMSO was distributed in 96-well plates. Different concentrations (10 mM–10 µM) of each complex were dissolved in DMSO and added in triplicate (50 µL) to a final concentration of 2.5 mM–2.5 µM per well. The control contained water or DMSO. The formation of β-hematin was initiated by the addition of acetate buffer (100 µL, 0.2 M, pH 4.4). The plates were incubated at 37 °C for 48 h and then centrifuged. After removing the supernatant, the precipitate was washed twice with DMSO and finally dissolved in NaOH (200 µL, 0.2 N). After diluting with NaOH (0.1 N), the absorbance was measured at 405 nm in a spectrophotometer. The inhibition of β-hematin was calculated in comparison with the negative control, and plotted against drug concentration generated using GraphPad Prism 5.01. Three independent experiments were performed.

2.13 CM-H2-DCFDA staining of *P. falciparum*

A volume of 100 µL of trophozoites of *P. falciparum* 3D7 strain at 3.0% parasitemia and 1.0% hematocrit in RPMI was dispensed per well in a 96-well round bottom plate. A volume of 25 µL of CM-H2-DCFDA (Life) at 15 µM suspended in medium was added to each well and incubated in the dark for 20 min. Then, 100 µL of drugs previously suspended in RPMI was added to the respective wells. Each drug concentration was tested in triplicate. The untreated parasites received 100 µL of medium containing 0.5% DMSO. The plates were incubated for 3.5 h at 37 °C under 3% O₂, 5% CO₂, 91% N₂ atmosphere. The plates were centrifuged at 1500 rpm for 5 min, the supernatant was discarded and 200 µL of isoton diluent was added and the samples were analyzed in a flow cytometer (LSRFortessa, BD). The gate of the infected cells was determined in comparison with the uninfected control. At least 200,000 events were acquired in the fluorescein isothiocyanate channel (488, 585 nm) for CM-H2-DCFDA. The analysis was performed using FlowJo (LLC) in three independent experiments.

2.14 Mitotracker and SYBR staining of *P. falciparum*

One hundred µL of rings of *P. falciparum* 3D7 strain at 2% parasitemia and 1.0% hematocrit in RPMI was dispensed in a 96-well round bottom plate. Then, 100 µL of drugs previously

suspended in RPMI was added to the respective wells. Each drug concentration was tested in triplicate. The untreated parasite received 100 µL of medium containing 0.5% DMSO. The plates were incubated for 24 h and 48 h at 37 °C under 3% O₂, 5% CO₂, 91% N₂ atmosphere. The plate was centrifuged with 200 µL of drug-free medium at 1500 rpm for 5 min and then 150 µL of mitotracker deep red FM (Life) at 5.0 µM and SYBRgreenI (at 2.5× suspended in medium) were added to each well and incubated in the dark for 30 min. After washing and adding 400 µL of isoton diluent, the samples were analyzed in a flow cytometer (LSRFortessa, BD). The gate of the infected cells was determined in comparison with the uninfected control. At least 200,000 events were acquired in the allophycocyanin channel (633, 660 nm) for mitotracker and the fluorescein isothiocyanate channel (488, 585 nm) for SYBR. Analysis was performed using FlowJo (LLC). Three independent experiments were recorded.

2.15 Transmission electron microscopy

Aliquots (3 mL) of trophozoites of *P. falciparum* 3D7 strain at 8% parasitemia and 5.0% hematocrit in RPMI were dispensed in a flask and treated with chloroquine or WV-90 at 5.0 µM and incubated for 5 h. The untreated culture received DMSO. After centrifugation twice, the cells were fixed with 2% formaldehyde and 2.5% glutaraldehyde (Electron Microscopy Sciences, Hatfield, PA) in sodium cacodylate buffer (0.1 M, pH 7.2) for 40 min at room temperature. After fixation, the cells were washed 3 times with cacodylate buffer and post-fixed with a 1.0% solution of osmium tetroxide containing 0.8% potassium ferrocyanide (Sigma-Aldrich) for 1 h. The cells were subsequently dehydrated in increasing concentrations of acetone (30, 50, 70, 90 and 100%) for 10 min in each step and embedded in Polybed resin (PolyScience family, Warrington, PA). Ultrathin sections on copper grids were contrasted with uranyl acetate and lead citrate. Micrographs were taken using a JEM-1230 microscope (JEOL, Peabody, MA).

2.16 *In vivo* activity (Peters test)²⁵

Male Swiss mice were infected by intraperitoneal injection of 1 × 10⁶ NK65 strain *P. berghei*-infected erythrocytes per mouse and randomly divided into groups of *n* = 5. Each drug was solubilized in DMSO/saline (20 : 80 v/v) prior to administration. Treatment was initiated 3 h post infection and given once a day for four consecutive days by intraperitoneal injection of 100 µL. Chloroquine-treated mice were used as a positive control group, while untreated infected mice receiving DMSO/saline were used as a negative control group. The following parameters were evaluated: parasitemia counted at 4, 5, 6 and 7 days post-infection and 30 days post-infection animal survival. Thin blood smears were prepared, fixed and stained with quick panoptic stain (Laborclin), while animal survival was observed daily. The % of parasitemia reduction was calculated as follows: [(mean vehicle group – mean treated group)/mean vehicle group] × 100. Two independent experiments were performed. For a transmission electron microscopy analysis, infected mice (*n* = 1/group) at 10 days post-infection (parasitemia at 16%) received a single dose of CQ or

WV-90 at $66 \mu\text{mol kg}^{-1}$ by an intraperitoneal route. Euthanasia was performed 6 h post treatment and the blood samples were taken and fixed for morphological study as described above.

2.17 *In vivo* activity (Thompson test)²⁶

Male Swiss mice were infected by intraperitoneal injection of 2×10^6 NK65 strain *P. berghei*-infected erythrocytes. At day 3 post-infection, mice with parasitemia up to 1.0% were randomly divided into groups of $n = 6$. Each drug was solubilized in DMSO/saline (20:80 v/v) and treatment was initiated at day 3 post infection and given daily for three consecutive days by intraperitoneal injection of 100 μL . Untreated infected mice receiving DMSO/saline were used as a negative control group. The following parameters were evaluated: parasitemia counted at day 8 post-infection and 30 days post-infection animal survival. Two independent experiments were performed.

2.18 Activity against *P. berghei* liver stage

Inhibition of hepatic infection was determined by measuring the luminescence intensity in the Huh-7 cells infected with a firefly luciferase-expressing *P. berghei* line as previously described.²⁷ Briefly, the Huh-7 cells were cultured in RPMI-1640 at pH 7.0 and maintained at 37 °C with 5% CO₂. For infection assays, the Huh-7 cells (1.0×10^4 per well) were seeded in 96-well plates the day before drug treatment and infection. The medium was replaced by medium containing the appropriate concentration of each compound approximately 1 h prior to infection with sporozoites freshly obtained through disruption of salivary

glands of infected female *Anopheles stephensi* mosquitoes. An amount of DMSO solvent equivalent to that present in the highest compound concentration was used as a control. Sporozoite addition was followed by centrifugation at 1700g for 5 min. Parasite infection load was measured 48 h after infection by a bioluminescence assay (Biotium, Hayward, CA). The effect of the compounds on the viability of Huh-7 cells was assessed by the AlamarBlue assay (Life), using the manufacturer's protocol.

2.19 Statistical analyses

Nonlinear regression analysis was used to calculate the CC₅₀, LC₅₀ and IC₅₀ values by using GraphPad Prism version 5.01 (Graph Pad Software, San Diego, CA). ANOVA, Newman-Keuls Multiple Comparison Test, Bonferroni post-test and log-rank (Mantel-Cox) test were employed in the indicated experiments. It was considered statistically significant when $p < 0.05$ as analyzed by GraphPad Prism version 5.01.

3. Results

The structures of the platinum(II)-chloroquine complexes with the general formula [PtCl(P)₂(CQ)]PF₆ [where (P)₂ = triphenylphosphine (PPh₃) (WV-92), 1,3-bis(diphenylphosphine)propane (dppp) (WV-90), 1,4-bis(diphenylphosphine)butane (dppb) (WV-93), 1,1'-bis(diphenylphosphine)ferrocene (dppf) (WV-94) and CQ = chloroquine] are shown in Fig. 1 along with the [PtCl₂(dppp)] (WV-48) complex, which is a chemical precursor of complex WV-90 lacking chloroquine in its composition.

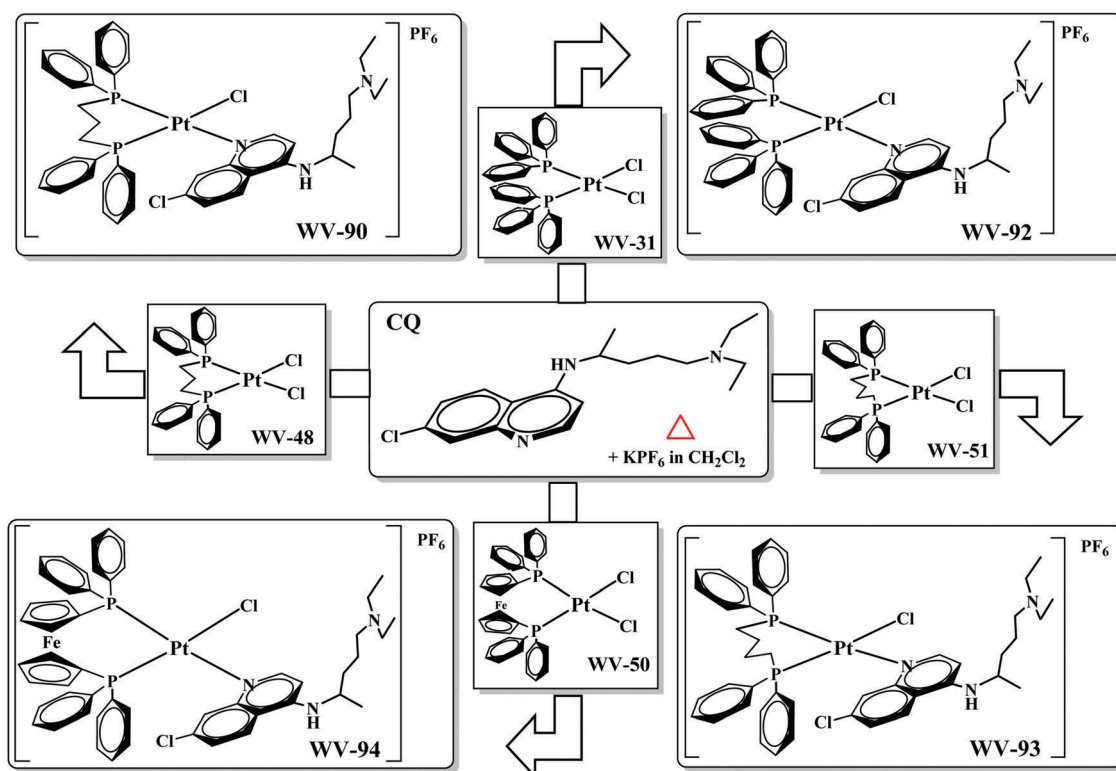


Fig. 1 Chemical structures of chloroquine and its platinum complexes.

All the complexes were previously characterized by physical and spectroscopies techniques.²² The characterization of the platinum(II) chloroquine complexes indicates that CQ binds to the metal center through the quinolinic nitrogen, and all the compounds displayed an axial chirality, generated by the rotation of the Pt–N bond (atropisomerism) which, combined with the chirality of the carbon C1' in the chloroquine ligand, produced a pair of diastereomers. The stability of the platinum(II)–chloroquine complexes was verified at room temperature by ³¹P{¹H} NMR spectroscopy in Tris–HCl solution containing 60% of DMSO. After 216 h, the spectra of the complexes remained similar when compared with those recorded using fresh solutions (Fig. S1, ESI†).

The *in vitro* activity was determined against the blood stage of *P. falciparum* 3D7 and W2 strains and response was given as mean IC₅₀ values. In parallel, *in vitro* cytotoxicity was performed in J774 and HepG2 cell lines and expressed as mean CC₅₀ values. Selectivity indexes were calculated for both parasite strains versus J774 cells (Table 1).

Chloroquine had an IC₅₀ value of 0.11 ± 0.035 μM against the chloroquine-sensitive *P. falciparum* 3D7 strain. The platinum complexes were approximately three times less active than chloroquine, except for WV-92 which was five times less active. Chloroquine had an IC₅₀ value of 0.43 ± 0.09 μM against the chloroquine-resistant *P. falciparum* W2 strain. Platinum complexes WV-90 and WV-94 were as active as chloroquine, while WV-92 and WV-93 were two-fold less active. None of the chloroquine-lacking complexes inhibited parasite growth up to 2.0 μM (Table S1, ESI†). Regarding cytotoxicity, gentian violet displayed CC₅₀ values of 14.2 ± 0.3 and 4.3 ± 0.8 μM for J774 and HepG2 cell lines, respectively. The platinum complexes and chloroquine were less cytotoxic than gentian violet. In comparison with chloroquine, the platinum complex WV-93 was equally cytotoxic to J774 cells, while other platinum complexes were approximately twice as cytotoxic. Selectivity indexes revealed that none of the platinum complexes was as selective as chloroquine. The platinum complexes WV-90 and WV-93 were respectively the most potent and selective among them and were selected for further investigation.

Table 1 Cytostatic activity of platinum complexes against intraerythrocytic *P. falciparum*, mammalian cell cytotoxicity and selectivity indexes

Comp.	<i>P. falciparum</i> , IC ₅₀ ± S.E.M. ^a (μM)		Cells, CC ₅₀ ± S.E.M. ^b (μM)		Selectivity index ^c	
	CQ-sensitive 3D7	CQ-resistant W2	J774	HepG2	3D7	W2
WV90	0.38 ± 0.06	0.5 ± 0.07	39.6 ± 4.3	87.4 ± 1.2	104	79
WV92	0.6 ± 0.01	0.7 ± 0.2	17.9 ± 2.4	35.5 ± 1.7	29	25
WV93	0.32 ± 0.02	0.76 ± 0.10	78.1 ± 1.7	58.5 ± 2.8	244	102
WV94	0.41 ± 0.1	0.5 ± 0.06	21.5 ± 1.0	29.3 ± 0.4	52	43
CQ	0.11 ± 0.035	0.43 ± 0.09	76.1 ± 3.1	37.6 ± 3.6	690	190
GV	—	—	14.2 ± 0.3	4.3 ± 0.8	—	—

^a Determined 48 h after incubation with compounds. ^b Determined 72 h after incubation with compounds. ^c Determined as CC₅₀ (J774 cells)/IC₅₀. Values were calculated as mean of three independent experiments. Abbreviations: CQ = chloroquine. GV = Gentian violet. IC₅₀ = inhibitory concentration at 50%. CC₅₀ = cytotoxic concentration at 50%. S.E.M = standard error of the mean.

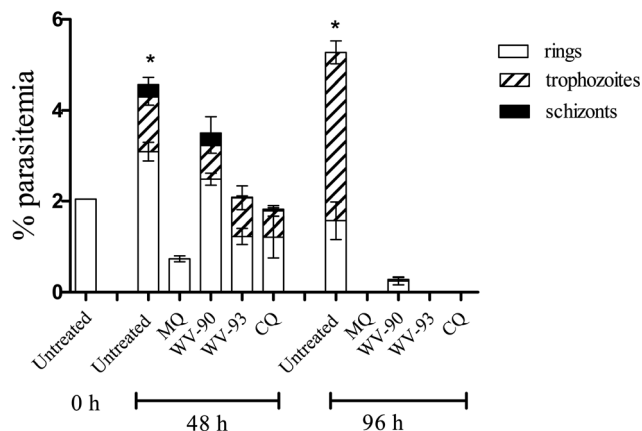


Fig. 2 Platinum complexes impair cell cycle development. 3D7 strain *P. falciparum* at the ring stage (2% parasitemia, 2.5% hematocrit) were incubated with vehicle (untreated), 0.6 μM of platinum compounds and 0.25 μM of CQ at 0 and 48 h. Mefloquine tested at 0.1 μM was used as a positive control. Quantification of each parasite stage at 48 and 96 h after the addition of the compounds is shown. Error bars represent standard deviation (S.D.) from triplicates of one experiment. Two independent experiments were determined. * *p* < 0.05 (one-way ANOVA and Newman–Keuls test) for parasitemia versus untreated 0 h. Abbreviations: CQ = chloroquine. MQ = mefloquine.

To examine the activity of the platinum complexes on the intraerythrocytic cell cycle, synchronous cultures of *P. falciparum* (3D7 strain) were incubated for 48 and 96 h in the presence of approximately twice the IC₅₀ concentration of each compound and mefloquine was used as a positive control. The growth of rings, trophozoites and schizonts was quantified by microscopy and the results were compared to untreated controls (Fig. 2). After 48 h incubation, untreated parasites developed from rings to trophozoites and a few schizonts, while mefloquine treatment completely abrogated development of ring into trophozoites. WV-90 reduced parasitemia but did not inhibit the parasite's cell cycle, while treatment with WV93 or chloroquine delayed parasite development from rings to trophozoites. Treatment for 96 h with WV-90 stopped the parasite cell cycle, with only a few parasites remaining in the ring stage. Similar to mefloquine, WV-93 and chloroquine treatment for 96 h completely abrogated the cell cycle.

The *in vitro* cytotoxic activity expressed as the drug concentration to achieve cytotoxicity (LC₅₀) was determined in parasites synchronized into the trophozoite stage of W2 strain, treated for 18 h prior to incubation for 48 h in the absence of the compounds (Table 2). Artesunate was used as the positive control and presented LC₅₀ in the nanomolar range, while chloroquine exhibited LC₅₀ values in the low micromolar range. For the platinum complexes, the LC₅₀ was approximately twice as high as the concentration required to inhibit parasite growth (IC₅₀). This is in agreement with the cell cycle experiment shown in Fig. 2, where the used concentration (twice the IC₅₀) inhibited cell cycle development by probably causing irreversible alteration in the parasites, acting like a parasitocidal drug. Under this same experimental condition, we estimated the minimal parasitocidal concentration (MPC). Artesunate presented MPC of 0.19 μM.

Table 2 Parasitocidal activity of platinum complexes against intraerythrocytic W2 strain of *P. falciparum*

Compounds	LC ₅₀ ± S.E.M. ^a (μM)	MPC ^b (μM)
WV-90	0.84 ± 0.03	5.0
WV-93	1.0 ± 0.2	10
CQ	0.43 ± 0.03	> 10
Artesunate	0.0049 ± 0.0009	0.19

^a After 18 h of exposure, the compounds were removed by extensive washing and parasite growth was quantified by hypoxanthine incorporation relative to untreated controls. LC₅₀ = lethal concentration at 50%. ^b MPC = minimal parasitocidal concentration.

From three independent experiments, chloroquine tested in concentrations up to 10 μM did not inhibit 100% parasite growth, while the platinum complex WV-90 at a concentration of 5.0 μM was able to eliminate the parasite. Of note, WV-90 did not induce hemolysis at concentrations below 12.5 μM (Fig. S2, ESI[†]), showing a parasite clearance activity without affecting erythrocyte integrity.

The primary target for the antimalarial quinolones like chloroquine in the intra-erythrocytic life stage is the ferriprotoporphyrin and its polymerization product, known as hemozoin (synthetic analog, β-hematin).^{8,10} A series of experiments targeting ferriprotoporphyrin (hemin) and heme aggregation (β-hematin) were performed. Titration of ferriprotoporphyrin was monitored using the Soret band of porphyrin and the perturbations upon increasing concentration of the compounds (Fig. 3). By using titration, we estimated the association constant (log *K*) of the compounds for ferriprotoporphyrin (Table 3). It was observed that in comparison with chloroquine, the complexes displayed a weaker interaction with ferriprotoporphyrin, where

WV-90 showed the highest association constant among the complexes. The inhibition of polymerization of hemin into β-hematin was characterized in the solid state by using infrared. The spectra of hemin and its spontaneous polymerization in acid buffer were monitored by the presence of signals at 1660 and 1210 cm⁻¹, which correspond to the formation of the iron-carboxylate bonds (Fig. 4A). Adding chloroquine and platinum complexes inhibited the formation of β-hematin, due to the absence of signal at 1660 and 1210 cm⁻¹ (Fig. 4B). In contrast, adding primaquine, both signals regarding β-hematin formation are observed, which can be explained since this anti-malarial compound has an extra-erythrocytic action mechanism.⁸ Furthermore, the inhibition of polymerization of hemin into β-hematin was studied in solution by UV-vis. As observed by IC₅₀ values (Table 3), WV-90 exhibited the best inhibition of β-hematin among the platinum(II)-chloroquinones, with a potency similar to that of chloroquine. In contrast, WV-92, which was the least active antiparasitic complex among them, presented the lowest ability to inhibit β-hematin formation. The metal complex lacking chloroquine, WV-48, did not inhibit hemin formation in solution at concentrations up to 2.0 mM (data not shown).

The ability of the platinum complexes to induce oxidative stress in trophozoites was assayed by flow cytometry using CM-H2-DCFDA, a general probe for reactive oxygen species (ROS). Fig. 5 (panel A) shows that, in comparison to untreated trophozoites, chloroquine increased the content of ROS in a concentration-dependent manner (significance, *p* < 0.05). At the same concentration range, however, neither WV-90 nor WV-93 increased ROS production in a concentration-dependent manner (no statistical significance). In addition, the platinum complex lacking chloroquine WV-48, which is devoid of

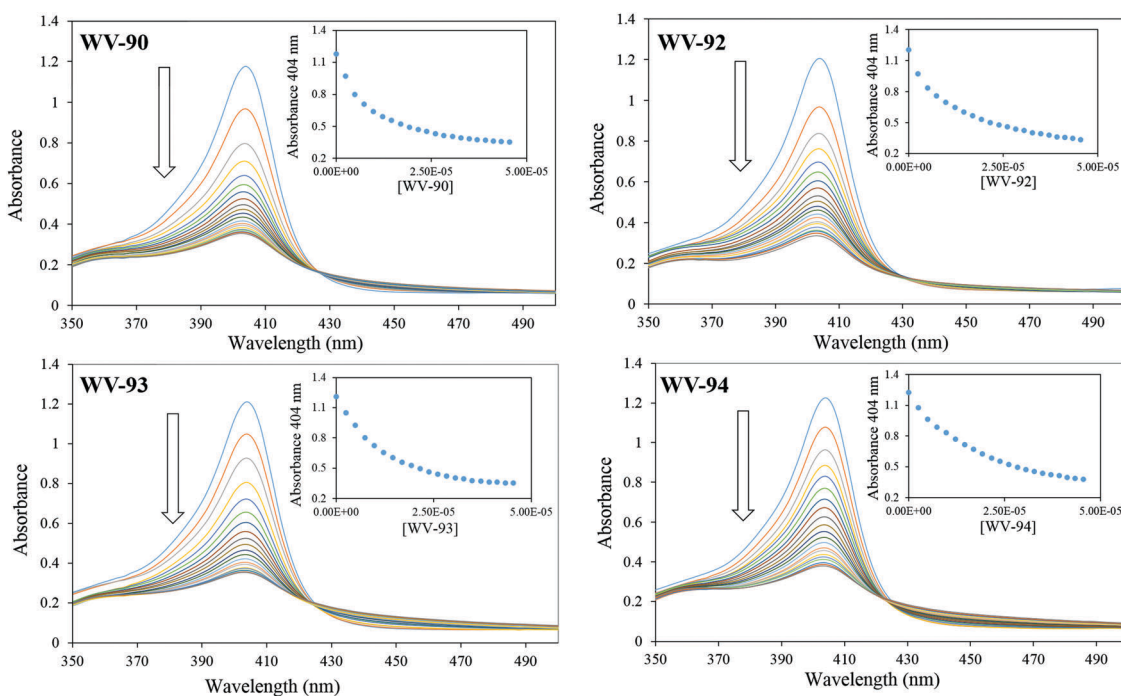


Fig. 3 Spectroscopic titration of ferriprotoporphyrin (Fe^{III}PPIX) with the platinum(II)-chloroquine complexes at pH 7.5.

Table 3 Hemin association constant and inhibition of β -hemin formation for platinum(II)-chloroquine complexes and chloroquine

Comp.	Hemin	β -Hematin	
	$\log K$	Presence of peaks at 1660 and 1210 cm^{-1}	$\text{IC}_{50} \pm \text{S.D.}^a$ (mM)
WV-90	5.11 ± 0.02	Not	0.24 ± 0.01
WV-92	4.95 ± 0.02	Not	0.34 ± 0.04
WV-93	4.95 ± 0.08	Not	0.27 ± 0.01
WV-94	4.70 ± 0.02	Not	0.27 ± 0.01
CQ	5.30 ± 0.08	Not	0.30 ± 0.04
PQ	N.D.	Yes	N.D.

Abbreviations: CQ = chloroquine. PQ = primaquine. N.D. = not determined. ^a Determined 48 h after incubation with compounds. K = association constant.

antiparasitic activity, increased ROS. Based on this, there was no evidence of a relationship between cellular ROS and antiparasitic activity for the platinum complexes. Next, we sought to study their effect on mitochondrial activity. To this end, untreated and treated trophozoites were co-stained with MitoTracker deep red (a probe for mitochondrial activity) and SYTO 61 (a nucleic acid staining) and analyzed by flow cytometry (Fig. 5, panels B and C). In comparison with untreated parasites, treatment with 2.5 μM of chloroquine or WV90 for 24 h reduced mitochondria staining by approximately 50%, while as observed by SYTO 61 staining, there was not substantial decrease in the parasitemia. When the parasites were incubated

for 48 h, reduction in both mitochondria activity and parasitemia was observed under treatment with 2.5 μM of chloroquine or WV-90, but the reduction of mitochondria activity was greater than the reduction in parasitemia under WV-90 treatment. Of note, these same effects were not observed under WV-48 treatment.

The onset of ultrastructural changes induced in trophozoites of the 3D7 strain of *P. falciparum* by chloroquine and WV-90 treatment was examined by transmission electron microscopy (Fig. 6). In untreated trophozoites, granules of electron dense hemozoin are observed in the peripheral cytoplasm or inside digestive vacuoles, usually containing a single and large hemozoin crystal. In comparison with the untreated control, chloroquine-treated parasites presented numerous but small hemozoin granules after 5 h of drug exposure. A hallmark of chloroquine treatment is the presence of digestive vacuoles with loss of material, characteristic of autophagosome formation. In the WV-90-treated parasites, in addition to numerous and small hemozoin granules, we observed large vesicles along the cytoplasm, which is suggestive of ribosomes depletion. In fact, depletion of ribosomes is a structural change observed before autophagosome formation. Swollen mitochondria were observed in chloroquine treatment, while loss of mitochondrial material was observed under WV-90 treatment. After determining the onset of ultrastructural changes *in vitro*, we further studied the ultrastructural effects *in vivo* by using *P. berghei* parasites collected from mice treated with a single dose of 66 $\mu\text{mol kg}^{-1}$

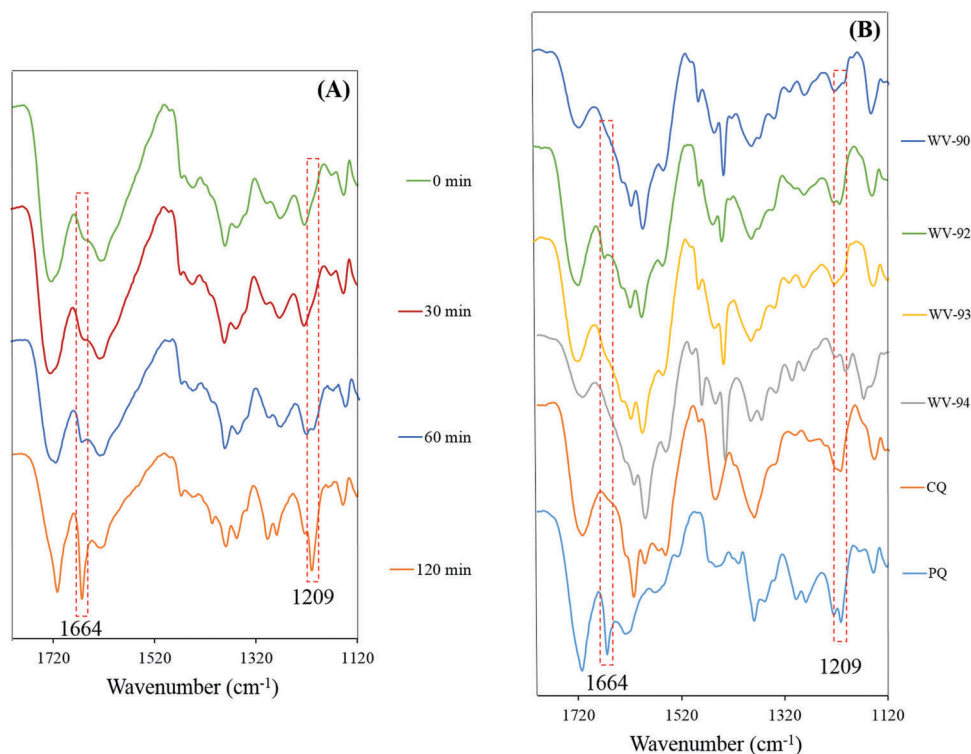


Fig. 4 (A) Infrared spectra of hemin after 0, 30, 60 and 120 min of incubation in acid buffer; (B) product of heme aggregation in the presence of 3 equivalents (mol mol^{-1}) of platinum complexes, chloroquine (CQ) or primaquine (PQ) after 120 min of incubation. In both panels, the red dotted lines indicate the bands for β -hemin formation.

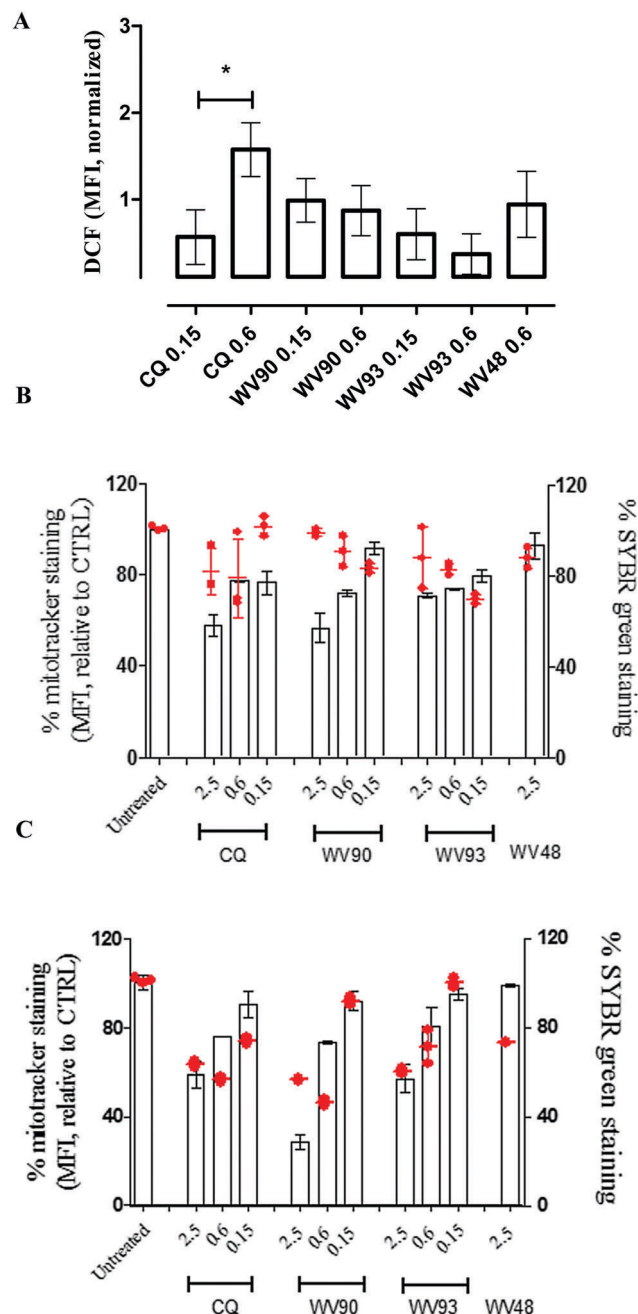


Fig. 5 Platinum complexes display phenotype effects on mitochondrial activity. 3D7 strain *P. falciparum* trophozoites were stained with DCF (panel A), mitotracker red (bars) and SYBRgreenI (red dots) (panels B and C). Compounds (concentration at μM) were incubated for 4 h (A), 24 h (B) and 48 (C) and analyzed by flow cytometry. Median fluorescence intensity (MFI) was normalized from the untreated control and obtained from pooling data gathered from three independent experiments. Error bars represent S.E.M. * $p < 0.05$ (one-way ANOVA and Newman–Keuls test).

of chloroquine or WV-90 (Fig. S3, ESI†). In comparison with the untreated control, chloroquine treatment resulted in parasites with enlarged digestive vacuoles, typical autophagosome formation and absence of electron dense hemozoin. Under WV-90 treatment, parasites displayed enlarged vacuoles, in some of which there was little electron dense hemozoin and undigested

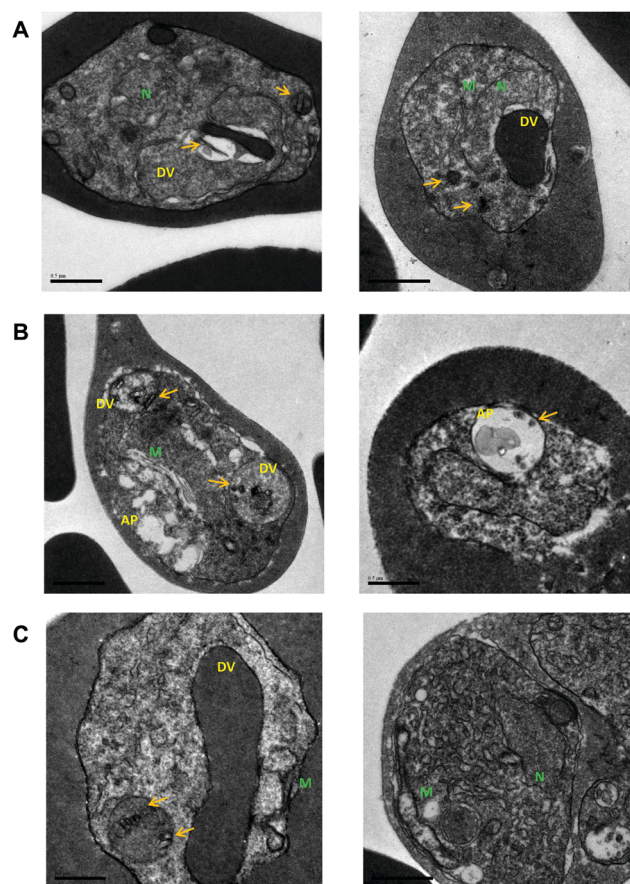


Fig. 6 Ultrastructural effects of platinum complex and chloroquine on 3D7 strain *P. falciparum* trophozoites. Representative transmission electron micrographs of untreated (panel A), chloroquine at $5.0 \mu\text{M}$ (panel B) and WV-90 at $5.0 \mu\text{M}$ (panel C) after 5 h of incubation. Abbreviation: N, nucleus, M, mitochondria; DV, digestive vacuole, AP, autophagosome. Arrows indicate hemozoin.

hemoglobin vesicles. Loss of mitochondrial material was also observed; however, unlike the *in vitro* experiment, WV-90 treatment in the *in vivo* experiment resulted in the formation of autophagosome vesicles.

Once the *in vitro* activity against the blood stage was assayed, we performed *in vivo* studies in mice. In a set of experiments, we determined the suppressive activity of parasitemia in NK65 strain *P. berghei*-infected mice using the Peters' protocol of 4 day treatment regime. Compounds were administered *via* the intraperitoneal route once a day and the ensuing parasitemia was determined by comparing to that of untreated mice by using data points from day 7 post-infection, while survival was determined up to 30 days post-infection. Upon analysis of the dose–response curve for chloroquine, a minimal dose to reduce 100% parasitemia and mortality of $66 \mu\text{mol kg}^{-1} \text{day}^{-1}$ was estimated (Fig. 7). Having ascertained the range of doses, we assessed the suppressive activity of the WV-90 and WV-93 complexes. When a dose of $66 \mu\text{mol kg}^{-1} \text{day}^{-1}$ was provided, the suppressive activity of WV-93 was approximately 1.2-fold lower than that of chloroquine, while the efficacy of WV-90 treatment was equipotent to that of chloroquine. The observed

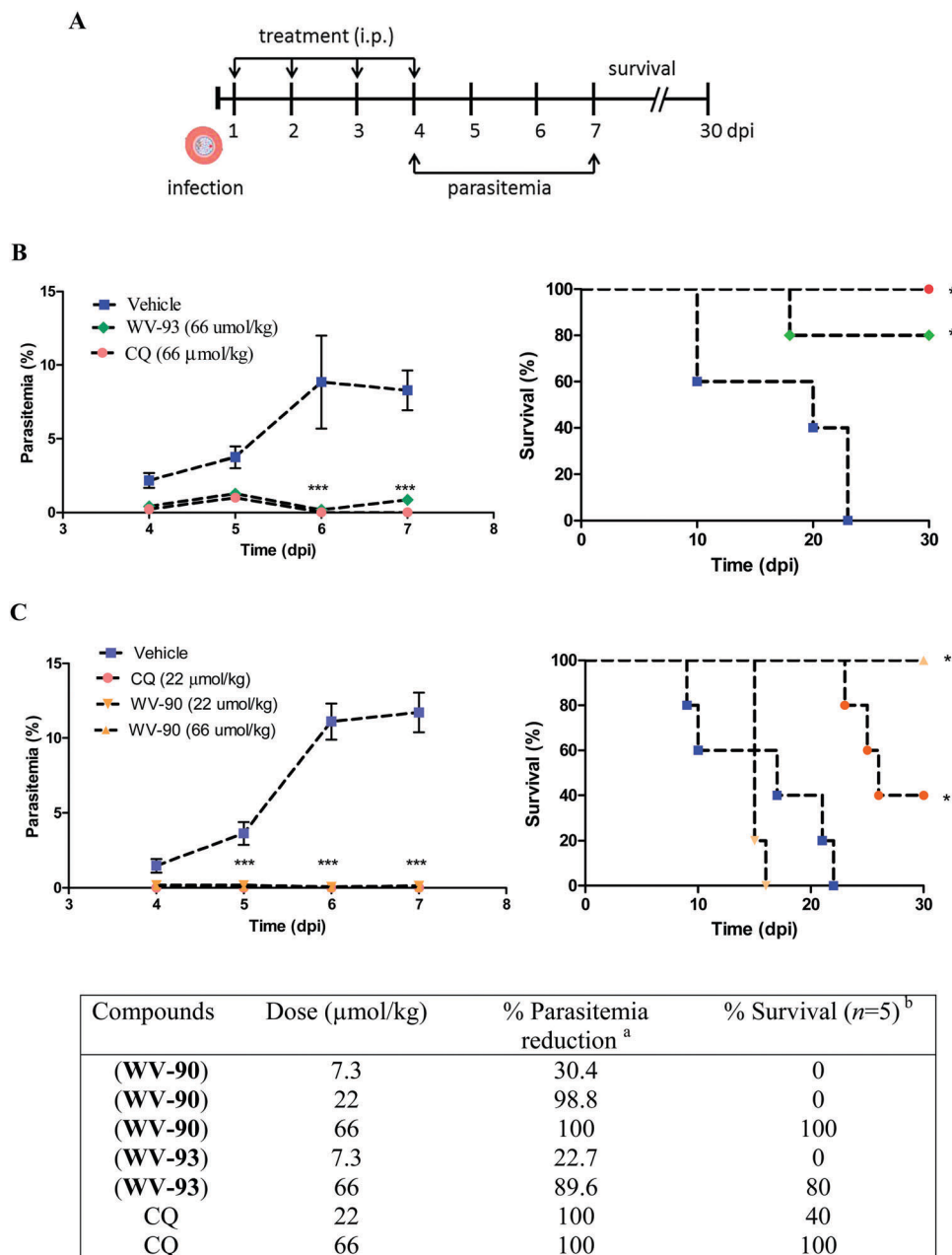


Fig. 7 Platinum complexes display suppressive activity. Experimental design of the Peters test (A), parasitemia and animal survival for WV-93 (B), WV-90 (C) and summary of dose–response curve (table). Infection by NK65 strain *P. berghei* in Swiss mice ($n = 5/\text{group}$). In panels (B and C), the values represent the mean of one experiment, the error bars represent S.D. *** $p < 0.01$ versus vehicle (two-way ANOVA and Bonferroni post-test), * $p < 0.05$ versus vehicle (log-rank and Mantel-Cox test). In panel (D), ^a by using data from day 7 post-infection. ^b Survival determined 31 dpi. Abbreviation: i.p., intraperitoneal; dpi, days post-infection; CQ, chloroquine.

suppression in parasitemia was reflected in the overall survival rates of treated mice, where treatment with chloroquine, WV-93 and WV-90 conferred 100, 80 and 100% survival, respectively. When a dose of $22 \mu\text{mol kg}^{-1} \text{day}^{-1}$ was administered, the suppressive activity of WV-90 treatment was the same as that of chloroquine. At this dose, WV-90 did not confer protection against mortality, while chloroquine provided 40% protection against mortality.

In another set of experiments, we evaluated the parasite clearance in an established *P. berghei* infection in mice using

the Thompson' protocol. In this regime, $66 \mu\text{mol kg}^{-1} \text{day}^{-1}$ of the compounds were administered by the intraperitoneal route for three consecutive days from days 3 to 5 post-infection and, on day 8 post-infection, the decrease in parasitemia was evaluated in comparison with the untreated group. Survival was determined up to 30 days post-infection (Fig. 8). The vehicle group presented a parasitemia of approximately 18% at day 8 post-infection, while chloroquine treatment led to clearance of parasites in the blood. Treatment with the WV-93 complex resulted in greater than 97% parasitemia reduction.

After clearance of parasitemia on day 8, recrudescence of infection was observed on day 14 for chloroquine and on day 17 for WV-93. As a result of the delay in the recrudescence of infection, mice treated with WV-93 presented a median survival time of 19.5 days, while for the untreated group and chloroquine group, the median survival times were 15.5 and 16 days, respectively. In two independent experiments, no mice were cured by chloroquine, whereas WV-93 treatment cured 25% of mice.

After ascertaining the activity against the blood stage, the activity of platinum complexes on *P. berghei* infection of Huh-7 cells was also evaluated (Fig. 9). In comparison with untreated controls, treatment with the WV-90 complex did not decrease the parasite load at the concentrations tested. In contrast, WV-93 reduced the parasite load by 50% at 10 μM , without affecting the viability of Huh-7 cells. The WV-93 complex displayed an IC_{50} of $10.88 \pm 0.68 \mu\text{M}$, while the IC_{50} of primaquine and chloroquine was approximately 10 and 15 μM , respectively.

4. Discussion

platinum(II)-chloroquines are water-stable compounds and represent a novel class of potential multistage antimalarial agents.

In vitro, the platinum complexes displayed antimalarial activity similar to chloroquine, even against a chloroquine-resistant *P. falciparum* strain. This activity is highly dependent on the presence of chloroquine in the composition of the metal complex. This was achieved with selectivity, without affecting mammalian and host cell viability. Importantly, the platinum complexes impaired parasite cell cycle development and presented irreversible parasiticidal effects.

The platinum complexes exhibited parasiticidal activity against trophozoites, where hemozoin formation is more active, which is part due to their inhibitory effects on β -hematin formation. Platinum compounds were as active as chloroquine, which is achieved due to the presence of chloroquine in their composition since the chloroquine-lacking complex was unable to inhibit hemozoin dimerization. However, chloroquine interacts with hemozoin more strongly than platinum complexes. Indeed, the free quinolonic nitrogen of chloroquine is not only considered crucial for cell-based activity but also for its interaction with hemozoin;^{9,10} in the platinum complexes, the quinolonic nitrogen is bound to a platinum atom. Based on this, it is suggested that their interaction with hemozoin is somewhat different than chloroquine. In agreement with this, we have demonstrated, by electron microscopy, that while there are marked similarities in the ultrastructural effects on parasites produced by both

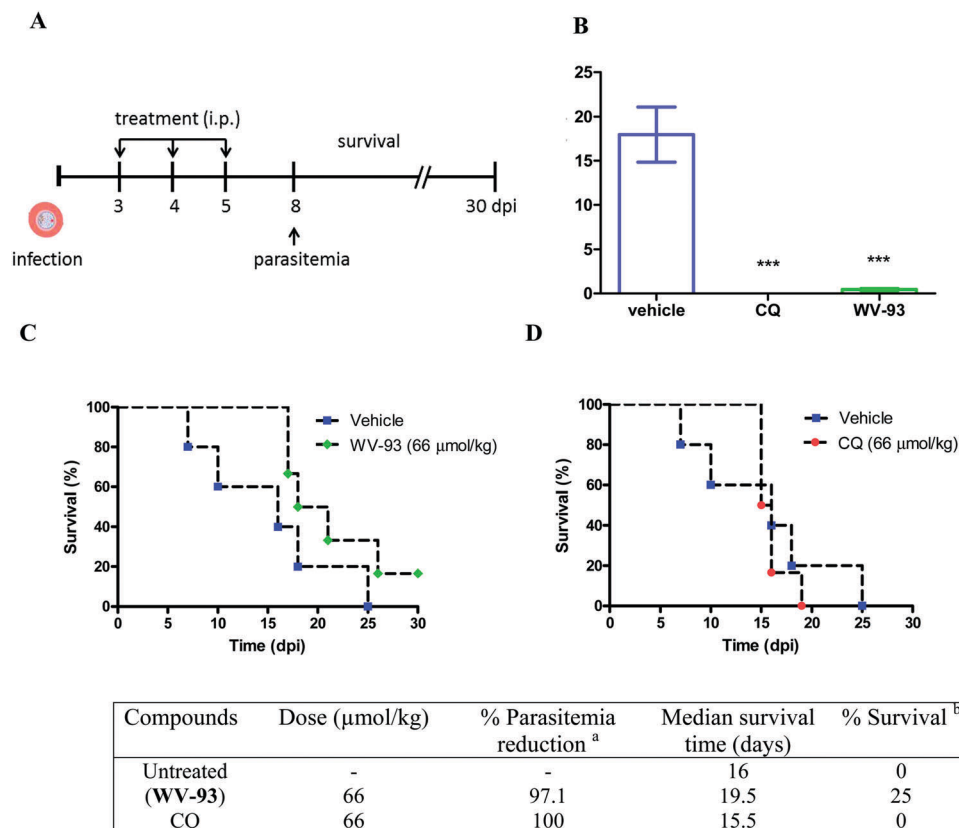


Fig. 8 Platinum complexes display clearance of parasitemia. Experimental design of the Thompson test (A), parasitemia (B), animal survival (C and D) and summary of dose-response curve (table). In panel (B), the values represent the mean \pm S.D. of one experiment. *** $p < 0.01$ versus vehicle (one-way ANOVA and Newman-Keuls test). ^b Survival determined 31 dpi by pooling data of two experiments. Abbreviation: i.p., intraperitoneal; dpi, days post-infection; CQ, chloroquine.

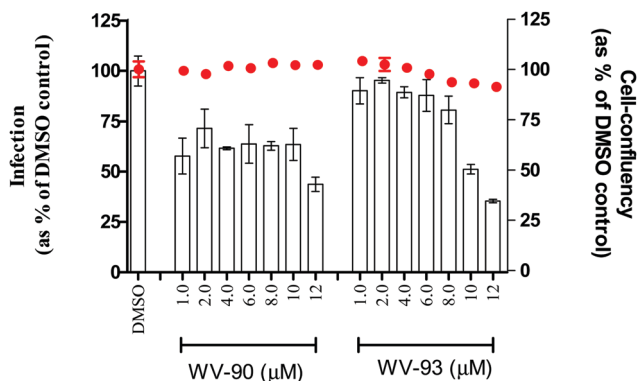


Fig. 9 Platinum complexes display activity against *P. berghei* sporozoites. Seeded Huh7 cells were treated with drugs and infected with sporozoites. Bioluminescence intensity was measured 48 h post-infection. Bars represent infection and red dots represent Huh7 cell confluency. Untreated control received only DMSO. Compound WV-93 presented $IC_{50} = 10.8 \pm 0.68 \mu\text{M}$. Error bars represent standard deviation from each concentration in triplicate. Results of one from two independent experiments.

chloroquine and the platinum complexes, chloroquine was more efficient in inhibiting hemozoin formation. Impairing hemozoin dimerization by chloroquine is known to result in incomplete hemoglobin digestion, starving the parasite of amino acids and therefore leading to the formation of autophagosome vesicles.²⁸ Unlike chloroquine, there was no evidence of autophagosome formation in parasites exposed *in vitro* to the platinum complexes. However, under *in vivo* experiments, the platinum complexes led to autophagosome vesicle formation. Although both *in vitro* and *in vivo* experiments had similar drug exposure times, the concentration that reaches parasite is different in each assay, in addition to the fact that under *in vivo* condition, the drugs may undergo biotransformation.

We further observed that, different from chloroquine, where hemozoin formation inhibition accumulates toxic heme and increases ROS, the platinum complexes inhibited hemozoin formation without increasing ROS in a concentration-dependent manner. In agreement with this, parasites treated with platinum complexes presented little but residual hemozoin crystals. The previously reported antimalarial organoruthenium–chloroquine complexes inhibited β -hematin formation and induced ROS which was even more pronounced than chloroquine.²¹ Collectively, these findings suggest that the nature of the transition metal can play an important role in the pharmacological profile of chloroquine–metal complexes, which is a common feature observed in the literature.^{29–31}

We observed by electron microscopy that the platinum complex-treated parasites exhibited loss of mitochondrial material. We further demonstrated that prior to impairment of parasite viability, the platinum complexes reduced mitochondrial activity within blood stage parasites. A variety of quinolines can act on lysosomal enzymes and coenzyme Q, involved in mitochondrial function.^{12,32} As such, the platinum compounds may interfere with the mitochondrial electron transport chain of the parasite. The platinum complexes were also active against *Plasmodium* exoerythrocytic stages. This was demonstrated by

the fact that, unlike chloroquine, the WV-93 complex possessed promising *in vitro* activity against the liver stage of *P. berghei*, supporting a potential for avoiding malaria relapse. The underlying mechanism for this activity is unknown. A number of compounds targeting *Plasmodium* liver stages are known to interfere with the mitochondrial electron transport chain.^{33,34} We observed that both chloroquine and WV-93 impaired mitochondrial activity and that a more pronounced effect was observed with the platinum complex. Based on this, the effects on the mitochondria of the platinum complex in the blood stage parasites may be the reason for the observed activity against liver stage malaria.

We further demonstrated that platinum complexes are effective *in vivo* against *P. berghei* in the suppressive activity model, despite its activity being not superior to that of chloroquine. In the clearance model of study (Thompson), mice in the platinum complex-treated group presented superior survival time than the chloroquine-treated group. Based on these data, the platinum complex has superior efficacy to chloroquine in the parasite clearance model. The platinum complexes were administered *via* an intraperitoneal route, which may represent a limitation in drug development. Nonetheless, in many cases treatment against severe malaria is given *via* an intravenous or intramuscular route until the patient can tolerate oral medication. Finally, mice exposed to the platinum compounds tolerated the complexes well, without signs of distress or discomfort, but evaluation of toxicological and pharmacokinetic studies is required in due course.

5. Conclusion

The incorporation of chloroquine into platinum compounds produced new antimalarial agents. They presented classical properties like chloroquine, such as activity against the blood stage, inhibitory activity against β -hematin and *in vivo* suppressive activity. However, unlike chloroquine, the platinum complexes reduced parasite load in the liver stage, and displayed irreversible trophozoite killing and an enhanced impairment of mitochondrial activity. In addition, promising *in vivo* curative effects were observed. Overall, our findings indicated that metal complexes combine the characteristics of chloroquine with possible novel effects due to the metal.

Conflicts of interest

The authors declare that there is no conflict of interest.

Acknowledgements

We are thankful to the flow cytometry facility of IGM (Brazil). This research was funded by Fundação de Amparo à Pesquisa do Estado da Bahia (grant PET0042/2013, Brazil), Fundação de Amparo à Pesquisa do Estado de São Paulo (grant 14/10516-7, Brazil) and Fundação para a Ciência e Tecnologia (grant PTDC/SAU-MIC/117060/2010, Portugal). D. R. M. M., A. A. B. and M. B. P. S. are recipients of fellowships from CNPq (Brazil).

References

- 1 R. E. Cibulskis, P. Alonso, J. Aponte, M. Aregawi, A. Barrette, L. Bergeron, C. A. Fergus, T. Knox, M. Lynch, E. Patouillard, S. Schwarte, S. Stewart and R. Williams, Malaria: Global progress 2000–2015 and future challenges, *Infect. Dis. Poverty*, 2016, **5**, 61, DOI: 10.1186/s40249-016-0151-8.
- 2 B. A. Willey, L. S. Paintain, L. Mangham, J. Car and J. A. Schellenberg, Strategies for delivering insecticide-treated nets at scale for malaria control: a systematic review, *Bull. W. H. O.*, 2012, **90**, 672E–684E, DOI: 10.2471/BLT.11.094771.
- 3 B. G. Koudou, H. Ghattas, C. Essé, C. Nsanzabana, F. Rohner, J. Utzinger, B. E. Faragher and A. B. Tschannen, The use of insecticide-treated nets for reducing malaria morbidity among children aged 6–59 months, in an area of high malaria transmission in central Côte d'Ivoire, *Parasites Vectors*, 2010, **3**, 91, DOI: 10.1186/1756-3305-3-91.
- 4 D. J. Kyabayinze, C. Asiimwe, D. Nakanjako, J. Nabakooza, H. Counihan and J. K. Tibenderana, Use of RDTs to improve malaria diagnosis and fever case management at primary health care facilities in Uganda, *Malar. J.*, 2010, **9**, 200, DOI: 10.1186/1475-2875-9-200.
- 5 N. W. Lucchi, F. Komino, S. A. Okoth, I. Goldman, P. Onyona, R. E. Wiegand, E. Juma, Y. P. Shi, J. W. Barnwell, V. Udhayakumar and S. Kariuki, *In vitro* and molecular surveillance for antimalarial drug resistance in *Plasmodium falciparum* parasites in western Kenya reveals sustained artemisinin sensitivity and increased chloroquine sensitivity, *Antimicrob. Agents Chemother.*, 2015, **59**, 7540–7547, DOI: 10.1128/AAC.01894-15.
- 6 L. Tilley, J. Straimer, N. F. Gnädig, S. A. Ralph and D. A. Fidock, Artemisinin action and resistance in *Plasmodium falciparum*, *Trends Parasitol.*, 2016, **32**, 682–696, DOI: 10.1016/j.pt.2016.05.010.
- 7 A. Pyae Phy, E. A. Ashley, T. J. Anderson, Z. Bozdech, V. I. Carrara, K. Sriprawat, S. Nair, M. M. White, J. Dziekan, C. Ling, S. Proux, K. Konghahong, A. Jeeyapant, C. J. Woodrow, M. Imwong, R. McGready, K. M. Lwin, N. P. Day, N. J. White and F. Nosten, Declining efficacy of artemisinin combination therapy against *P. falciparum* malaria on the Thai-Myanmar border (2003–2013): the role of parasite genetic factors, *Clin. Infect. Dis.*, 2016, **63**, 784–791, DOI: 10.1093/cid/ciw388.
- 8 T. J. Egan, D. C. Ross and P. A. Adams, Quinoline anti-malarial drugs inhibit spontaneous formation of beta-haematin (malaria pigment), *FEBS Lett.*, 1994, **352**, 54–57, DOI: 10.1016/0014-5793(94)00921-X.
- 9 I. Weissbuch and L. Leiserowitz, Interplay between malaria, crystalline hemozoin formation, and antimalarial drug action and design, *Chem. Rev.*, 2008, **108**, 4899–4914, DOI: 10.1021/cr078274t.
- 10 T. J. Egan, Recent advances in understanding the mechanism of hemozoin (malaria pigment) formation, *J. Inorg. Biochem.*, 2008, **102**, 1288–1299, DOI: 10.1016/j.jinorgbio.2007.
- 11 J. Krungkrai, The multiple roles of the mitochondrion of the malarial parasite, *Parasitology*, 2004, **129**, 511–524, DOI: 10.1017/S0031182004005888.
- 12 A. M. Stickles, L. M. Ting, J. M. Morrisey, Y. Li, M. W. Mather, E. Meermeier, A. M. Pershing, I. P. Forquer, G. P. Miley, S. Pou, R. W. Winter, D. J. Hinrichs, J. X. Kelly, K. Kim, A. B. Vaidya, M. K. Riscoe and A. Nilsen, Inhibition of cytochrome bc1 as a strategy for single-dose, multi-stage antimalarial therapy, *Am. J. Trop. Med. Hyg.*, 2015, **92**, 1195–1201, DOI: 10.4269/ajtmh.14-0553.
- 13 M. Fry and M. Pudney, Site of action of the antimalarial hydroxynaphthoquinone, 2-[*trans*-4-(4'-chlorophenyl) cyclohexyl]-3-hydroxy-1,4-naphthoquinone (566C80), *Biochem. Pharmacol.*, 1992, **43**, 1545–1553, DOI: 10.1016/0006-2952(92)90213-3.
- 14 J. E. Siregar, G. Kurisu, T. Kobayashi, M. Matsuzaki, K. Sakamoto, F. Mi-ichi, Y. Watanabe, M. Hirai, H. Matsuoka, D. Syafruddin, S. Marzuki and K. Kita, Direct evidence for the atovaquone action on the *Plasmodium* cytochrome bc1 complex, *Parasitol. Int.*, 2015, **64**, 295–300, DOI: 10.1016/j.parint.2014.09.011.
- 15 M. L. Hovlid and E. A. Winzeler, Phenotypic screens in antimalarial drug discovery, *Trends Parasitol.*, 2016, **32**, 697–707, DOI: 10.1016/j.pt.2016.04.014.
- 16 L. M. Birkholtz, T. L. Coetzer, D. Mancama, D. Leroy and P. Alano, Discovering new transmission-blocking antimalarial compounds: challenges and opportunities, *Trends Parasitol.*, 2016, **32**, 669–681, DOI: 10.1016/j.pt.2016.04.017.
- 17 A. S. Ressurreição, D. Gonçalves, A. R. Siteo, I. S. Albuquerque, J. Gut, A. Góis, L. M. Gonçalves, M. R. Bronze, T. Hanscheid, G. A. Biagini, P. J. Rosenthal, M. Prudêncio, P. O'Neill, M. M. Mota, F. Lopes and R. Moreira, Structural optimization of quinolon-4(1*H*)-imines as dual-stage antimalarials: toward increased potency and metabolic stability, *J. Med. Chem.*, 2013, **56**, 7679–7690, DOI: 10.1021/jm4011466.
- 18 A. Gomes, B. Pérez, I. Albuquerque, M. Machado, M. Prudêncio, F. Nogueira, C. Teixeira and P. Gomes, *N*-Cinnamoylation of antimalarial classics: quinacrine analogues with decreased toxicity and dual-stage activity, *ChemMedChem*, 2014, **9**, 305–310, DOI: 10.1002/cmdc.201300459.
- 19 H. Kaur, M. Machado, C. de Kock, P. Smith, K. Chibale, M. Prudêncio and K. Singh, Primaquine-pyrimidine hybrids: synthesis and dual-stage antiplasmodial activity, *Eur. J. Med. Chem.*, 2015, **101**, 266–273, DOI: 10.1016/j.ejmech.2015.06.045.
- 20 M. Mushtaque and Shahjahan, Reemergence of chloroquine (CQ) analogs as multi-targeting antimalarial agents: a review, *Eur. J. Med. Chem.*, 2015, **90**, 280–295, DOI: 10.1016/j.ejmech.2014.11.022.
- 21 T. S. Macedo, L. C. Vegas, M. Paixão, M. Navarro, B. C. Barreto, P. C. M. Oliveira, S. G. Macambira, M. Machado, M. Prudêncio, S. D'Alessandro, N. Basilico, D. R. M. Moreira, A. A. Batista and M. B. P. Soares, Chloroquine-containing organoruthenium complexes are fast-acting multistage antimalarial agents, *Parasitology*, 2016, **143**, 1543–1556, DOI: 10.1017/S0031182016001153.
- 22 W. Villarreal, L. Colina-Vegas, C. Rodrigues de Oliveira, J. C. Tenorio, J. Ellena, F. C. Gozzo, M. R. Cominetti, A. G. Ferreira, M. A. Ferreira, M. Navarro and A. A. Batista., Chiral

- platinum(II) complexes featuring phosphine and chloroquine ligands as cytotoxic and monofunctional DNA-binding agents, *Inorg. Chem.*, 2015, **54**, 11709–11720, DOI: 10.1021/acs.inorgchem.5b01647.
- 23 T. J. Egan, W. W. Mavuso, D. C. Ross and H. M. Marques, Thermodynamic factors controlling the interaction of quinoline antimalarial drugs with ferriprotoporphyrin IX, *J. Inorg. Biochem.*, 1997, **68**, 137–145, DOI: 10.1016/S0162-0134(97)00086-X.
- 24 S. Parapini, N. Basilico, E. Pasini, T. J. Egan, P. Olliaro, D. Taramelli and D. Monti, Standardization of the physico-chemical parameters to assess *in vitro* the beta-hematin inhibitory activity of antimalarial drugs, *Exp. Parasitol.*, 2000, **96**, 249–256, DOI: 10.1006/expr.2000.4583.
- 25 W. Peters, The chemotherapy of rodent malaria, XXII. The value of drug-resistant strains of *P. berghei* in screening for blood schizontocidal activity, *Ann. Trop. Med. Parasitol.*, 1975, **69**, 155–171, DOI: 10.1080/00034983.1975.11686997.
- 26 A. L. Ager, in Experimental models: rodent malaria models (*in vivo*), ed. W. Peters and W. H. G. Richards, *Handbook of experimental pharmacology: antimalarial drugs*, Springer-Verlag, New York, N.Y., 1997, vol. 68, pp. 225–254.
- 27 I. H. Ploemen, M. Prudêncio, B. G. Douradinha, J. Ramesar, J. Fonager, G. J. van Gemert, A. J. Luty, C. C. Hermsen, R. W. Sauerwein, F. G. Baptista, M. M. Mota, A. P. Waters, I. Que, C. W. Lowik, S. M. Khan, C. J. Janse and B. M. Franke-Fayard, Visualisation and quantitative analysis of the rodent malaria liver stage by real time imaging, *PLoS One*, 2009, **4**, e7881, DOI: 10.1371/journal.pone.0007881.
- 28 P. R. Totino, C. T. Daniel-Ribeiro, S. Corte-Real and M. F. Ferreira-da-Cruz, *Plasmodium falciparum*: erythrocytic stages die by autophagic-like cell death under drug pressure, *Exp. Parasitol.*, 2008, **118**, 478–486, DOI: 10.1016/j.exppara.2007.10.017.
- 29 E. Ekengard, L. Glans, I. Cassells, T. Fogeron, P. Govender, T. Stringer, P. Chellan, G. C. Lisensky, W. H. Hersh, I. Doverbratt, S. Lidin, C. de Kock, P. J. Smith, G. S. Smith and E. Nordlander, Antimalarial activity of ruthenium(II) and osmium(II) arene complexes with mono- and bidentate chloroquine analogue ligands, *Dalton Trans.*, 2015, **44**, 19314–19329, DOI: 10.1039/c5dt02410b.
- 30 N. B. Souza, A. C. Aguiar, A. C. Oliveira, S. Top, P. Pigeon, G. Jaouen, M. O. Goulart and A. U. Krettli, Antiplasmodial activity of iron(II) and ruthenium(II) organometallic complexes against *Plasmodium falciparum* blood parasites, *Mem. Inst. Oswaldo Cruz*, 2015, **110**, 981–988, DOI: 10.1590/0074-02760150163.
- 31 S. Tapanelli, A. Habluetzel, M. Pellei, L. Marchiò, A. Tombesi, A. Capparè and C. Santini, Novel metalloantimalarials: Transmission blocking effects of water soluble Cu(I), Ag(I) and Au(I) phosphane complexes on the murine malaria parasite *Plasmodium berghei*, *J. Inorg. Biochem.*, 2017, **166**, 1–4, DOI: 10.1016/j.jinorgbio.2016.10.004.
- 32 S. C. Teguh, N. Klonis, S. Duffy, L. Lucantoni, V. M. Avery, C. A. Hutton, J. B. Baell and L. Tilley, Novel conjugated quinoline-indoles compromise *Plasmodium falciparum* mitochondrial function and show promising antimalarial activity, *J. Med. Chem.*, 2013, **56**, 6200–6215, DOI: 10.1021/jm400656s.
- 33 F. P. Da Cruz, C. Martin, K. Buchholz, M. J. Lafuente-Monasterio, T. Rodrigues, B. Sönnichsen, R. Moreira, F. J. Gamo, M. Marti, M. M. Mota, M. Hannus and M. Prudêncio Drug, screen targeted at *Plasmodium* liver stages identifies a potent multistage antimalarial drug, *J. Infect. Dis.*, 2012, **205**, 1278–1286, DOI: 10.1093/infdis/jis184.
- 34 T. Rodrigues, F. P. da Cruz, M. J. Lafuente-Monasterio, D. Gonçalves, A. S. Ressurreição, A. R. Siteo, M. R. Bronze, J. Gut, G. Schneider, M. M. Mota, P. J. Rosenthal, M. Prudêncio, F. J. Gamo, F. Lopes and M. Moreira, Quinolin-4(1H)-imines are potent antiplasmodial drugs targeting the liver stage of malaria, *J. Med. Chem.*, 2013, **56**, 4811–4815, DOI: 10.1021/jm400246e.